

## Sensitization of Er luminescence by Si nanoclusters

M. Wojdak, M. Klik, M. Forcales, O. B. Gusev,\* and T. Gregorkiewicz

*Van der Waals-Zeeman Institute, University of Amsterdam, Valckenierstraat 65, NL-1018 XE Amsterdam, The Netherlands*

D. Pacifici, G. Franzò, and F. Priolo

*MATIS-INFM and Dipartimento di Fisica e Astronomia, Università di Catania, Via Santa Sofia 64, I-95123 Catania, Italy*

F. Iacona

*CNR-IMM; Sezione di Catania, Stradale Primosole 50, I-95121 Catania, Italy*

(Received 22 March 2004; published 30 June 2004)

Sensitization of Er emission by Si nanoclusters (Si-nc) is investigated with pulsed and continuous optical pumping, in and off resonance with excited states of  $\text{Er}^{3+}$  ion. We show that under high-power pulsed pumping, the excitation process is limited by the finite energy transfer time from Si-nc to  $\text{Er}^{3+}$  ions. By comparison between pulsed and steady-state excitation, the concentration of sensitizers and average number of  $\text{Er}^{3+}$  ions coupled to a single nanocluster are independently determined in an experiment. The results clarify conditions needed for efficient sensitization of  $\text{SiO}_2\text{:Er}$  by Si-nc.

DOI: 10.1103/PhysRevB.69.233315

PACS number(s): 78.55.-m, 31.70.Hq, 78.67.Bf, 81.07.Bc

Due to a spectroscopically sharp and temperature-stable radiative transition at  $\lambda \approx 1.54 \mu\text{m}$  which coincides with a minimum loss in optical fibers, the  $\text{Er}^{3+}$  ion is the optical dopant of choice for optoelectronic applications.<sup>1</sup> Semiconductor hosts are especially attractive for optical doping. The photoluminescence (PL) excitation cross section is in this case very high due to an efficient band-to-band absorption. Unfortunately, for Er-doped crystalline Si nonradiative de-excitation processes lead to thermal quenching of  $\text{Er}^{3+}$  emission.<sup>2</sup> On the other hand, in a dielectric like  $\text{SiO}_2$ , which provides good thermal stability of  $\text{Er}^{3+}$  PL, its excitation efficiency is low, as only resonant energy absorption by the  $\text{Er}^{3+} 4f$  electron core is possible. To combine the advantages of both hosts, a different type of Si-based Er-doped optical medium was recently explored. It is comprised of an Er-doped  $\text{SiO}_2$  matrix in which a high concentration of silicon nanoclusters (Si-nc) is dispersed.<sup>3</sup> Nanocrystalline materials are currently investigated for the realization of optical gain.<sup>4</sup> The Si-nc mediated energy transfer offers an effective excitation cross section of  $\sim 10^{-16} \text{ cm}^2$ ,<sup>5,6</sup> much higher than the  $10^{-21} - 10^{-19} \text{ cm}^2$  cross section of resonant excitation for  $\text{Er}^{3+}$  in  $\text{SiO}_2$ .<sup>5,7</sup>

In this heterogeneous medium ( $\text{SiO}_2\text{:Si-nc,Er}$ ) the incoming photons are captured in Si-nc due to efficient band-to-band absorption,<sup>8</sup> and subsequently, the excitation energy is transferred to  $\text{Er}^{3+}$  ions located preferably outside Si-nc.<sup>9,10</sup> In this way, an efficient channel for nonresonant excitation leading to temperature-stable  $\text{Er}^{3+}$  emission is realized. Moreover, electrical excitation can also be achieved and efficient electroluminescent devices have recently been demonstrated.<sup>11</sup> In the current study, we investigate in detail the sequential excitation mechanism of  $\text{Er}^{3+}$  ions in  $\text{SiO}_2\text{:Si-nc:Er}$ . In particular, we show that under certain excitation conditions, the emission is limited by the concentration of Si-nc coupled to  $\text{Er}^{3+}$  ions.

The experiments were performed on two Er-doped silica samples ( $\text{SiO}_2\text{:Er}$ ) of which one also contained Si nanoclusters ( $\text{SiO}_2\text{:Si-nc:Er}$ ). The Si-nc were fabricated by annealing

(1250°C, 1 h) of a 0.1  $\mu\text{m}$  thick film of  $\text{SiO}_x$  with 42 at. % Si, grown on a quartz substrate by plasma enhanced chemical vapor deposition.<sup>5</sup> By using a transmission electron microscope coupled with an electron energy loss spectrometer tuned to the energy of the plasmon in Si (16.7 eV), the total concentration of Si-nc was found to be  $5 \times 10^{17} - 1 \times 10^{18} \text{ cm}^{-3}$  with a mean diameter of  $d \approx 3.5 \text{ nm}$ . The uniform Er concentration of  $2.2 \times 10^{20} \text{ cm}^{-3}$  over the whole thickness of the films was obtained by multiple Er implantations at different doses and energies, followed by 1 h annealing at 900°C. We will refer to the  $\text{SiO}_2\text{:Er}$  and  $\text{SiO}_2\text{:Si-nc:Er}$  films as Sample Nos. 1 and 2, respectively.

The PL measurements were carried out at room temperature under pulsed and continuous (cw) pumping. As a pulsed source, a tunable optical parametric oscillator (OPO) was used, producing pulses of 5 ns duration at a 20 Hz repetition rate. By scanning the OPO wavelength, a PL excitation (PLE) study was performed. For cw pumping, the  $\lambda = 514.5 \text{ nm}$  and 476.5 nm lines of an  $\text{Ar}^+$  laser were used. The PL spectra were resolved with a single grating spectrometer and recorded with a germanium detector. The PL dynamics were measured with a near-infrared photomultiplier having a response time of 300 ns.

PL experiments showed that the  $\text{Er}^{3+}$  related emission, originating from the  ${}^4I_{13/2} \rightarrow {}^4I_{15/2}$  transition, has the same spectral shape for Samples Nos. 1 and 2 (not shown). The  $\text{Er}^{3+}$  ions in Sample No. 1 were excited resonantly with the OPO set to  $\lambda_{\text{exc}} = 520 \text{ nm}$ , while for Sample No. 2, an identical emission spectrum was obtained for a broad range of excitation wavelengths. We conclude that the  $\text{Er}^{3+}$  PL spectrum is not affected by the presence of Si-nc. In contrast to that, the introduction of nanoclusters reduces the lifetime of the  ${}^4I_{13/2}$  state from  $\tau_{\text{Er}}^{\text{SiO}_2} \approx 11 \text{ ms}$  to about  $\tau_{\text{Er}}^{\text{Si-nc}} \approx 3 \text{ ms}$ . The observed shortening of the decay time can be due to the reduction in radiative lifetime of the  ${}^4I_{13/2}$  excited state, induced by the change of refractive index in the heterogeneous medium.<sup>12</sup> By measuring the refractive index change upon introduction of Si-nc and assuming that the lifetime of  $\text{Er}^{3+}$

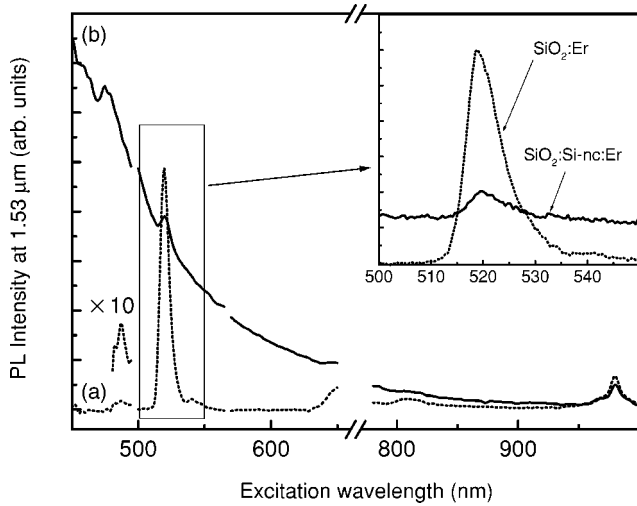


FIG. 1. Room-temperature photoluminescence excitation spectra for Sample No. 1 ( $\text{SiO}_2:\text{Er}$ ) (a) and Sample No. 2 ( $\text{SiO}_2:\text{Si-nc,Er}$ ) (b). Inset presents details of PLE spectra at  $\lambda_{\text{exc}} \approx 520$  nm, measured with maximum OPO power ( $\Phi \approx 3 \times 10^{25} \text{ cm}^{-2} \text{ s}^{-1}$ ).

in silica is purely radiative, we have estimated the radiative lifetime of  $\text{Er}^{3+}$  in Sample No. 2 as  $\sim 9$  ms. Therefore, any further decrease in the measured lifetime has to be ascribed to nonradiative de-excitation channels available in the matrix containing Si-nc. This leads to a reduction of the Er-related PL intensity by a factor of  $\sim 3$ , with respect to Er in  $\text{SiO}_2$ .

Figure 1 shows room-temperature excitation spectra of Er-related PL at  $\lambda = 1.53 \mu\text{m}$  for Sample Nos. 1 and 2. As can be seen, for  $\text{Er}^{3+}$  ions in  $\text{SiO}_2$  only resonant excitation is allowed with emission peaks corresponding to internal transitions within the  $4f$  electron core. The introduction of Si-nc (Sample No. 2) allows indirect excitation over a broad wavelength range.

The right panel of Fig. 1 shows details of PLE spectra around  $\lambda_{\text{exc}} \approx 520$  nm measured with the maximum available OPO power. It should be noted that the spectral width of the OPO is about 0.5 nm and therefore the measured broadening is not instrumental, but reflects the physical width of this PLE line.

Figure 2 presents the dependence of PL intensity (at  $\lambda = 1.53 \mu\text{m}$ ) as a function of excitation density. Displayed sets of points correspond to: (a) Sample No. 1 ( $\text{SiO}_2:\text{Er}$ ) excited at  $\lambda_{\text{exc}} = 520$  nm, (b) Sample No. 2 ( $\text{SiO}_2:\text{Si-nc,Er}$ ) excited at  $\lambda_{\text{exc}} = 520$  nm, where indirect and direct excitation channels are possible, and (c) Sample No. 2 excited at  $\lambda_{\text{exc}} = 510$  nm (indirect excitation only). Trace (d) represents the difference between the last two measurements and corresponds to the contribution of direct excitation in presence of Si-nc. The measurements were performed with the same experimental settings, thus the PL intensity scale is common for all the data points. As can be seen, the indirectly excited  $\text{Er}^{3+}$  emission from  $\text{SiO}_2:\text{Si-nc,Er}$  (c) saturates. This saturation level can be exceeded when also the direct excitation channel of  $\text{Er}^{3+}$  ions is enabled, by setting the OPO to  $\lambda_{\text{exc}} = 520$  nm (b). Apparently, when the indirect excitation channel saturates, direct excitation, despite its much smaller cross

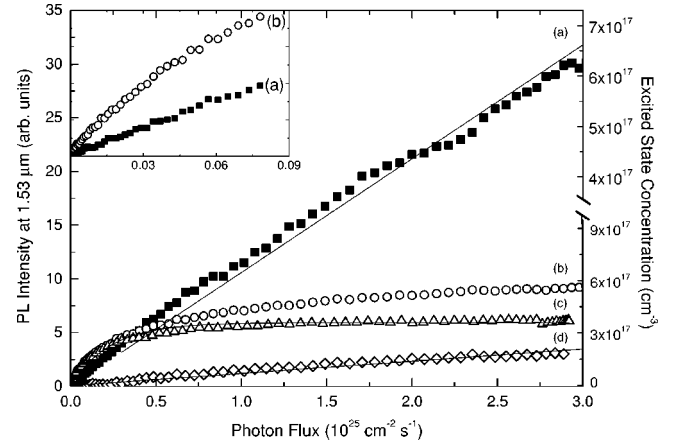


FIG. 2. Time-integrated PL intensity at  $\lambda = 1.53 \mu\text{m}$  as function of the pulsed excitation density: (a) Sample No. 1 ( $\text{SiO}_2:\text{Er}$ ) excited at  $\lambda_{\text{exc}} = 520$  nm, (b) Sample No. 2 ( $\text{SiO}_2:\text{Si-nc,Er}$ ) excited at  $\lambda_{\text{exc}} = 520$  nm, (c) Sample No. 2 excited at  $\lambda_{\text{exc}} = 510$  nm; (d) the difference between (b) and (c). The right-hand scale shows the concentration of  $\text{Er}^{3+}$  ions in the excited state in Sample No. 1 (upper part) and Sample No. 2 (lower part). The inset presents a detail for the low flux regime.

section, gives a sizeable PL contribution that increases linearly with the flux — trace (d). For small flux regime, far from saturation, both samples show an approximately linear dependence with the stronger emission from the Si-nc-doped sample, as shown in the inset to Fig. 2. We note that the enhancement due to Si-nc is only by a factor of  $\sim 3$ , and not  $10^2$  as usually reported from cw experiments.

For interpretation of these results, we use a simple two-stage model of  $\text{Er}^{3+}$  excitation. Since the duration of the OPO pulse ( $\Delta t = 5$  ns) is much shorter than the characteristic lifetime of  $\text{Er}^{3+}$  in the excited state  $\tau$ , we assume that recombination does not take place during illumination, and by the end of the pulse population  $N_{\text{Er}}^*$  reaches the level of:

$$N_{\text{Er}}^*(t = \Delta t) = N_{\text{Er}}^{\text{ex}} [1 - \exp(-\sigma \Phi \Delta t)], \quad (1)$$

where  $N_{\text{Er}}^{\text{ex}}$  is the total concentration of excitable  $\text{Er}^{3+}$  ions present in the sample,  $N_{\text{Er}}^*$  is the concentration of the ions in the excited state,  $\sigma$  is the effective excitation cross section, and  $\Phi$  is the photon flux. For low excitation density, when  $\sigma \Phi \Delta t \ll 1$ , this formula gives a linear dependence on flux:  $N_{\text{Er}}^*(t) = \sigma \Phi N_{\text{Er}}^{\text{ex}} \Delta t$ . On the other hand, when  $\sigma \Phi \Delta t \gg 1$ , we obtain saturation, as all the  $\text{Er}^{3+}$  ions participating in the process become excited:  $N_{\text{Er}}^* = N_{\text{Er}}^{\text{ex}}$ . In this measurement, the PL pulse is integrated in time; since PL emission is proportional to  $N_{\text{Er}}^* / \tau_{\text{rad}}$ , the result of the experiment is given by  $N_{\text{Er}}^* \tau / \tau_{\text{rad}}$ , where  $\tau$  and  $\tau_{\text{rad}}$  are effective and radiative lifetimes, respectively.

From Fig. 2, we conclude that the  $\text{SiO}_2:\text{Er}$  emission shows a linear dependence over the whole investigated flux range. In this case, the integrated PL intensity is proportional to  $\sigma N_{\text{Er}}^{\text{ex}} \Delta t \Phi (\tau / \tau_{\text{rad}})$ , and the values of these parameters are known:  $\sigma_{\text{SiO}_2:\text{Er}}^{520 \text{ nm}} = 2 \times 10^{-20} \text{ cm}^2$ ,  $N_{\text{Er}}^{\text{ex}} = 2.2 \times 10^{20} \text{ cm}^{-3}$  (all implanted ions are optically active), and  $\tau / \tau_{\text{rad}} = 1$  (we assume that nonradiative recombination of Er does not take

place). Therefore, the well-characterized SiO<sub>2</sub>:Er system can be used to attribute the PL intensity to a particular concentration of excited Er<sup>3+</sup> ions, as given by the upper right-hand scale in Fig. 2. Although the PL intensity scale is common for all data points in Fig. 2, the Er<sup>3+</sup> excited state population should be corrected for the Si-nc-induced change in radiative effective total lifetimes, which reduces the  $\tau/\tau_{\text{rad}}$  ratio by a factor of 3. Consequently, the excited state population in Sample No. 2 has to be three times higher in order to give PL intensity equal to that of Sample No. 1, in the same excitation conditions. This correction is included in the lower part of the right-hand scale in Fig. 2. We now conclude that the PL saturation observed for Sample No. 2 under indirect excitation corresponds to an excited Er<sup>3+</sup> concentration of about  $N_{\text{Er}}^{\text{ex}} \approx 3.6 \times 10^{17} \text{ cm}^{-3}$ , which is only a minor part of the total Er<sup>3+</sup> amount present in the sample. By fitting dataset (c) with Eq. (1), we determine the effective cross section of the Si-nc mediated excitation as  $\sigma = 8.7 \pm 0.3 \times 10^{-17} \text{ cm}^2$ , close to previous reports.<sup>5,6</sup> We note, that a similar value of  $\sigma$  can also be estimated from the general formula for excitation cross section of Er<sup>3+</sup> in crystalline Si.<sup>13</sup>

The contribution from the Er<sup>3+</sup> ions directly excited in Sample No. 2 is represented in Fig. 2 by points (d). The flux dependence of this emission is linear, similar to that for SiO<sub>2</sub>:Er — trace (a), but with a smaller slope. If the direct excitation cross section is assumed to be the same in both samples, the slope difference implies a reduction of the concentration of optically active ions. From this, we conclude that in SiO<sub>2</sub>:Er with Si-nc a sizeable percentage of Er<sup>3+</sup> ions can be optically nonactive. In the present case, in Sample No. 2 only ~30% of the total amount of Er<sup>3+</sup> contributes to the PL regardless of the excitation mode. Recent measurements indeed show that the active fraction of Er<sup>3+</sup> in presence of Si-nc varies upon thermal treatments.<sup>14</sup>

In the linear regime, the PL intensity ratio of Sample Nos. 2 and 1,  $I_2/I_1$  is given by

$$\frac{I_2}{I_1} = \frac{\sigma_2 \times N_2 (\tau_2 / \tau_2^{\text{rad}})}{\sigma_1 \times N_1 (\tau_1 / \tau_1^{\text{rad}})}, \quad (2)$$

where  $\sigma_{1,2}$ ,  $N_{1,2}$ ,  $\tau_{1,2}$  and  $\tau_{1,2}^{\text{rad}}$  correspond to the effective excitation cross section, concentration of excitable Er<sup>3+</sup> ions, effective, and radiative decay times, for the Sample Nos. 1 and 2, respectively. If we consider that upon the introduction of Si-nc, the excitation cross section is increased approximately  $4.3 \times 10^3$  times, the  $\tau/\tau_{\text{rad}}$  ratio is reduced by a factor of 3, and the Er<sup>3+</sup> population, which can be excited via Si-nc, is  $3.6 \times 10^{17} \text{ cm}^{-3}$ , then we obtain  $I_2/I_1 \approx 2.3$ . This is indeed observed in the linear regime of pulsed excitation, where the Si-nc sensitized emission is about three times stronger as shown in the inset in Fig. 2. To compare this with the PL intensity ratio observed for cw excitation with an Ar<sup>+</sup> laser, we should take into account that the  $\lambda_{\text{exc}} = 514.5 \text{ nm}$  line is not exactly resonant with the  $^4I_{15/2} \rightarrow ^2H_{11/2}$  transition at 520 nm. From the broadening of the SiO<sub>2</sub>:Er PLE line (Fig. 1), we see that the excitation cross section at 514.5 nm is about ten times smaller than at 520 nm. This fact will influence the PL intensity ratio in favor of Sample No. 2 and we get  $I_2/I_1 \approx 23$ . For the experiment with  $\lambda_{\text{exc}} = 488 \text{ nm}$  line of

the Ar<sup>+</sup> laser, the direct excitation cross section of Er<sup>3+</sup> for Sample No. 1 is about 30 times lower than at  $\lambda_{\text{exc}} = 520 \text{ nm}$  (as shown in Fig. 1), which leads to  $I_2/I_1 \approx 70$ . This rough estimation of PL intensity increase in Sample No. 2 is in good agreement with experimental reports on two orders of magnitude PL enhancement by Si-nc doping.<sup>3</sup> Therefore at this stage, we conclude that the reduced concentration of Er<sup>3+</sup> ions, which can be efficiently excited via Si-nc, can account for the moderate increase of PL intensity in SiO<sub>2</sub>:Si-nc sample.

However, it should be noted that the obtained saturation level of  $N_{\text{Er}}^{\text{ex}} \approx 3.6 \times 10^{17} \text{ cm}^{-3}$  is comparable with the concentration of Si-nc in Sample No. 2. While the excitation proceeds via Si-nc, it is also possible that the emission saturates due to Si-nc rather than Er<sup>3+</sup> ions. Indeed, with the photon flux of  $\Phi = 1 \times 10^{25} \text{ cm}^{-2} \text{ s}^{-1}$ , we get for the excitation rate of a nanocluster a value of  $\sigma \Phi = 10^9 \text{ s}^{-1}$ , where we have used the measured value  $\sigma = 1 \times 10^{-16} \text{ cm}^2$  for the excitation cross section of a Si nanocluster. Therefore, during the 5 ns of the laser pulse, each nanocluster is excited five times. It cannot, however, accumulate generated excitons due to a strong Auger effect which rapidly (~1 ns) reduces their number. We note, that although the nanocluster can transfer an exciton to a nearby Er<sup>3+</sup> ion, the transfer time is of the order of a microsecond,<sup>15,16</sup> i.e., much longer than the Auger time constant. This makes the Er<sup>3+</sup> excitation process non-competitive with Auger quenching. At the end of the laser pulse, only one exciton per nanocluster is left to transfer its energy to a nearby Er<sup>3+</sup> ion. Due to this mechanism, under pulsed pumping, the concentration of excited Er ions cannot exceed the concentration of Si-nc. In that way, the present measurements provide a possibility of direct experimental determination of the concentration of Si-nc sensitizers.

The above outlined PL saturation mechanism will not occur under cw pumping, where temporal limitations are of no importance and every nanocluster can undergo multiple excitations during illumination time. We hence performed cw measurements in and out of resonance using an excitation wavelength of 514.5 or 476.5 nm of an Ar<sup>+</sup> ion laser, respectively. The data reported in Fig. 3 show that, the 1.54  $\mu\text{m}$  PL intensity in Sample No. 2 increases linearly with excitation density for the flux range up to  $\Phi \approx 5 \times 10^{18} \text{ cm}^{-2} \text{ s}^{-1}$ . For higher flux values, excitation becomes less efficient (sublinear dependence) but no saturation is reached within the investigated range, up to  $\Phi = 10^{21} \text{ cm}^{-2} \text{ s}^{-1}$ . (The higher PL intensity at  $\lambda_{\text{exc}} = 476.5 \text{ nm}$  is ascribed to the larger absorption coefficient of Si-nc at shorter wavelengths.) Comparing the results obtained for both samples under 514.5 nm pumping in the linear regime, we conclude that the introduction of Si-nc leads to an increase of the steady-state PL by a factor of  $I_2/I_1$  of ~35–70. Within the experimental error, this is in reasonable agreement with the results obtained from the pulsed excitation experiments discussed earlier.

Since PL intensity from Sample No. 1 is practically a linear function of the photon flux, similarly as for the pulsed experiment, we can use this dependence to determine the concentration of the excited Er<sup>3+</sup> ions in Sample No. 2. In that way we conclude that the concentration of the Er<sup>3+</sup> ions which can be excited in Sample No. 2 under cw pumping exceeds the “saturation” level realized under pulsed pump-

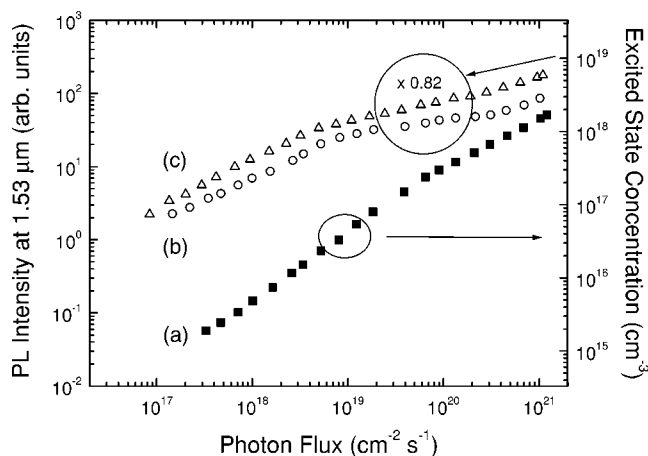


FIG. 3. PL intensity at  $\lambda=1.53 \mu\text{m}$  as a function of the continuous excitation density: (a) Sample No. 1 ( $\text{SiO}_2:\text{Er}$ ) excited at  $\lambda_{\text{exc}}=514.5 \text{ nm}$ , (b) Sample No. 2 ( $\text{SiO}_2:\text{Si-nc:Er}$ ) excited at  $\lambda_{\text{exc}}=514.5 \text{ nm}$  (in resonance), (c) Sample No. 2 excited at  $\lambda_{\text{exc}}=476.5 \text{ nm}$  (out of resonance), and the right-hand scale shows the concentration of  $\text{Er}^{3+}$  ions in the excited state attributed in Sample No. 1. Due to the lifetime difference, the concentration scale for Sample No. 2 should be corrected by 0.82, as indicated.

ing, by more than an order of magnitude. (The very high concentration of excited  $\text{Er}^{3+}$  ions is also confirmed by the upconversion, which occurs in this case.<sup>15</sup>)

The striking differences in results obtained for Sample No. 2 under pulsed and cw excitation can be readily understood when we assume that the saturation behavior observed in Fig. 2 is due to the limited concentration of sensitizers (Si-nc) rather than  $\text{Er}^{3+}$  ions. The linear regime in Fig. 3 ( $\Phi \leq 5 \times 10^{18} \text{ cm}^{-2} \text{ s}^{-1}$ ) will correspond then to the situation when one Si nanocluster can transfer energy to a single  $\text{Er}^{3+}$  ion only. In that range, the excitation process is characterized by the very high excitation cross section of  $\sigma \approx 10^{-16} \text{ cm}^2$ , but the number of  $\text{Er}^{3+}$  ions “excitable” in this way is equal

to the concentration of Si-nc acting as sensitizers. As the cw pumping density increases ( $\Phi > 5 \times 10^{18} \text{ cm}^{-2} \text{ s}^{-1}$ ) we step over to a regime when every nanocluster activates multiple  $\text{Er}^{3+}$  ions. Since the energy transfer time ( $\sim 1 \mu\text{s}$ ) is much shorter than the Er decay time ( $\sim 3 \text{ ms}$ ), the concentration of excited  $\text{Er}^{3+}$  ions builds up toward saturation.

By comparing the data of Fig. 3 with the saturation level determined in Fig. 2, we conclude that at the maximum flux, on average up to 20  $\text{Er}^{3+}$  ions are excited by a single Si nanocluster. In that way, the differences in results obtained under pulsed and cw excitation open the route for a deeper understanding of the microscopic details of the sensitization process.

In conclusion, the current findings provide the most direct illustration of the sequential character of the  $\text{SiO}_2:\text{Er}$  PL sensitized by Si-nc. Under high-power pulsed pumping every sensitizer can transfer energy to one  $\text{Er}^{3+}$  ion, and the excited state population stabilizes at a level equal to the concentration of Si nanoclusters active in the sensitization process. Such a measurement allows the direct experimental determination of the total concentration of sensitizing nanoclusters. Under intense cw pumping, the excitation process changes from a regime when every Si-nc excites at most one  $\text{Er}^{3+}$  ion (high excitation cross section) to a situation when excitation of several  $\text{Er}^{3+}$  ions originates from photon absorption in the same Si-nc (excitation cross section gradually decreases). It is therefore evident that careful simultaneous optimization of concentrations of both the emitting centers ( $\text{Er}^{3+}$  ions) and sensitizers (Si-nc) is required for realization of efficient emission and, possibly, optical gain in  $\text{SiO}_2:\text{Si-nc,Er}$ .

The work in Amsterdam was financially supported by the *Stichting voor Fundamenteel Onderzoek der Materie* (FOM), the Nederlandse Organisatie voor Wetenschappelijk Onderzoek (NWO), and by ARL European Research Office (ERO). The work in Catania was supported by EU through the IST-SINERGIA project and by MIUR through the FIRB project.

\*Permanent address: A.F. Ioffe Physico-Technical Institute, RAS, 194021 St. Petersburg, Russia.

<sup>1</sup>S. Schmitt-Rink, C. M. Varma, and A. F. J. Levi, *Phys. Rev. Lett.* **66**, 2782 (1991); S. S. Iyer and Y.-H. Xie, *Science* **260**, 40 (1993).

<sup>2</sup>F. Priolo, G. Franzò, S. Coffa, and A. Carnera, *Phys. Rev. B* **57**, 4443 (1998); P. G. Kik *et al.*, *Appl. Phys. Lett.* **70**, 1721 (1997).

<sup>3</sup>M. Fujii *et al.*, *Appl. Phys. Lett.* **71**, 1198 (1997); M. Fujii *et al.*, *J. Appl. Phys.* **84**, 4525 (1998); G. Franzò *et al.*, *Appl. Phys. A: Mater. Sci. Process.* **69**, 3 (1999); F. Priolo *et al.*, *Mater. Sci. Eng., B* **81**, 9 (2001); C. E. Chryssou *et al.*, *Appl. Phys. Lett.* **75**, 2011 (1999).

<sup>4</sup>L. Pavesi *et al.*, *Nature (London)* **408**, 440 (2000); V. I. Klimov *et al.*, *Science* **290**, 314 (2000).

<sup>5</sup>F. Priolo *et al.*, *J. Appl. Phys.* **89**, 264 (2001).

<sup>6</sup>A. J. Kenyon *et al.*, *J. Appl. Phys.* **91**, 367 (2002).

<sup>7</sup>W. J. Miniscalco, *J. Lightwave Technol.* **9**, 234 (1991).

<sup>8</sup>D. Kovalev, H. Hockler, M. Ben-Chorin, G. Polisski, M. Schwartzkopff, and F. Koch, *Phys. Rev. Lett.* **81**, 2803 (1998).

<sup>9</sup>X. L. Wu, V. F. Mei, G. G. Siu, K. L. Wong, K. Molding, M. J. Stokes, C. L. Fu, and X. M. Bao, *Phys. Rev. Lett.* **86**, 3000 (2001).

<sup>10</sup>G. Franzò *et al.*, *Appl. Phys. Lett.* **76**, 2167 (2000).

<sup>11</sup>F. Iacona *et al.*, *Appl. Phys. Lett.* **81**, 3242 (2002).

<sup>12</sup>E. Snoeks, A. Lagendijk, and A. Polman, *Phys. Rev. Lett.* **74**, 2459 (1995).

<sup>13</sup>O. B. Gusev, M. S. Bresler, P. E. Pak, I. N. Yassievich, M. Forcales, N. Q. Vinh, and T. Gregorkiewicz, *Phys. Rev. B* **64**, 075302 (2001).

<sup>14</sup>G. Franzò *et al.*, *Appl. Phys. Lett.* **82**, 3871 (2003).

<sup>15</sup>D. Pacifici, G. Franzò, F. Priolo, F. Iacona, and L. Dal Negro, *Phys. Rev. B* **67**, 245301 (2003).

<sup>16</sup>K. Watanabe *et al.*, *J. Appl. Phys.* **90**, 4761 (2001).